

# Commissioning of a Combined Hot-Streak and Swirl Profile Generator in a Transonic Turbine Test Facility

**Maxwell G. Adams**

Department of Engineering Science,  
University of Oxford,  
Parks Road,  
Oxford OX1 3PJ, UK

**Thomas Povey**

Department of Engineering Science,  
University of Oxford,  
Parks Road,  
Oxford OX1 3PJ, UK

**Benjamin F. Hall**

Department of Engineering Science,  
University of Oxford,  
Parks Road,  
Oxford OX1 3PJ, UK

**David N. Cardwell**

Department of Engineering Science,  
University of Oxford,  
Parks Road,  
Oxford OX1 3PJ, UK

**Kam S. Chana**

Department of Engineering Science,  
University of Oxford,  
Parks Road,  
Oxford OX1 3PJ, UK

**Paul F. Beard<sup>1</sup>**

Department of Engineering Science,  
University of Oxford,  
Parks Road,  
Oxford OX1 3PJ, UK  
e-mail: paul.beard@eng.ox.ac.uk

*By enhancing the premixing of fuel and air prior to combustion, recently developed lean-burn combustor systems have led to reduced NO<sub>x</sub> and particulate emissions in gas turbines. Lean-burn combustor exit flows are typically characterized by nonuniformities in total temperature, or so-called hot-streaks, swirling velocity profiles, and high turbulence intensity. While these systems improve combustor performance, the exiting flow-field presents significant challenges to the aerothermal performance of the downstream turbine. This paper presents the commissioning of a new fully annular lean-burn combustor simulator for use in the Oxford Turbine Research Facility (OTRF), a transonic rotating facility capable of matching nondimensional engine conditions. The combustor simulator can deliver engine-representative turbine inlet conditions featuring swirl and hot-streaks either separately or simultaneously. To the best of our knowledge, this simulator is the first of its kind to be implemented in a rotating turbine test facility. The combustor simulator was experimentally commissioned in two stages. The first stage of commissioning experiments was conducted using a bespoke facility exhausting to atmospheric conditions (Hall and Povey, 2015, "Experimental Study of Non-Reacting Low NO<sub>x</sub> Combustor Simulator for Scaled Turbine Experiments," ASME Paper No. GT2015-43530.) and included area surveys of the generated temperature and swirl profiles. The survey data confirmed that the simulator performed as designed, reproducing the key features of a lean-burn combustor. However, due to the hot and cold air mixing process occurring at lower Reynolds number in the facility, there was uncertainty concerning the degree to which the measured temperature profile represented that in OTRF. The second stage of commissioning experiments was conducted with the simulator installed in the OTRF. Measurements of the total temperature field at turbine inlet and of the high-pressure (HP) nozzle guide vane (NGV) loading distributions were obtained and compared to measurements with uniform inlet conditions. The experimental survey results were compared to unsteady numerical predictions of the simulator at both atmospheric and OTRF conditions. A high level of agreement was demonstrated, indicating that the Reynolds number effects associated with the change to OTRF conditions were small. Finally, data from the atmospheric test facility and the OTRF were combined with the numerical predictions to provide an inlet boundary condition for numerical simulation of the test turbine stage. The NGV loading measurements show good agreement with the numerical predictions, providing validation of the stage inlet boundary condition imposed. The successful commissioning of the simulator in the OTRF will enable future experimental studies of lean-burn combustor–turbine interaction. [DOI: 10.1115/1.4044224]*

## Introduction

Turbine inlet profiles are changing as a result of a shift from rich-burn to lean-burn combustion systems in aero-engine gas turbines to reduce NO<sub>x</sub> emissions. In particular, the circumferential temperature nonuniformity at the exit of modern lean-burn combustors is generally weaker because of enhanced mixing generated by swirlers, through which the primary combustion air is injected. A prominent radial temperature nonuniformity still exists, caused by the near-wall dilution flows, which act to cool the platforms. Furthermore, residual swirl persists downstream of the combustion zone and presents at turbine inlet.

Nonuniformities in the turbine inlet profiles are known to affect turbine aerodynamics, heat transfer, and therefore stage performance, and thus, there is a need for experimental data in order to

understand the impact of lean-burn combustors on the high-pressure (HP) and subsequent turbine stages. Measurements of these impacts within an engine are made challenging by the harsh flow conditions experienced. This has led to the use of scaled turbine test facilities, such as the Oxford Turbine Research Facility (OTRF), in order to obtain measurements at engine-representative conditions.

Several published studies report the design, development, and implementation of combustor simulators that reproduce certain turbine inlet nonuniformities for scaled turbine experiments. A comprehensive review of these developments is given by Povey and Qureshi [1]. The first hot-streak or overall temperature distortion factor (OTDF) generator for use in the OTRF was reported by Chana et al. [2]. A second-generation enhanced OTDF (enhanced overall temperature distortion function (EOTDF)) generator was later developed by Povey and Qureshi [3] to provide a turbine inlet temperature distortion representative of an extreme operating point in a modern engine cycle. In both systems, cold gas was introduced into a hot mainstream flow via radial and

<sup>1</sup>Corresponding author.

Manuscript received January 25, 2019; final manuscript received July 1, 2019; published online January 29, 2020. Assoc. Editor: Marc D. Polanka.

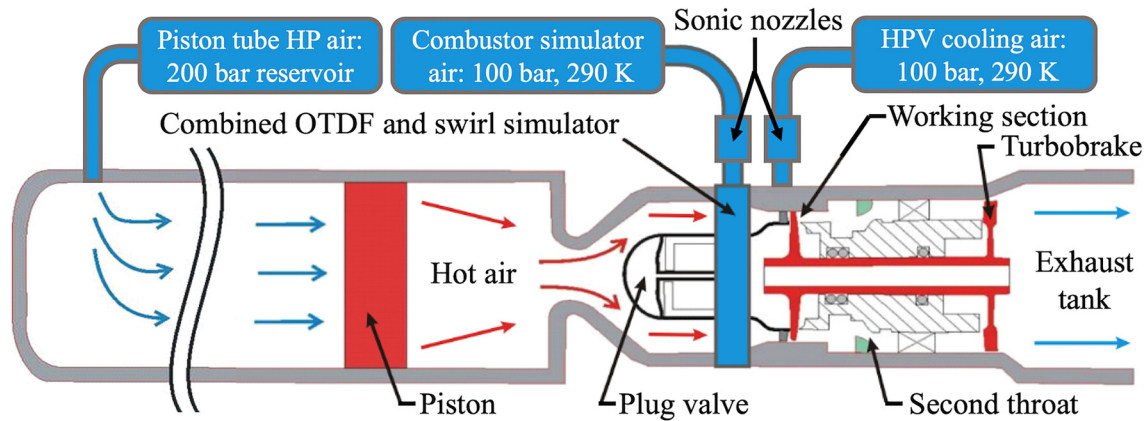


Fig. 1 Schematic of the OTRF

circumferential slots upstream of the turbine stage. Accurate area survey measurements of the simulated temperature profile showed pronounced radial and circumferential nonuniformities that were nondimensionally well matched to the target profile. High degrees of both pitch-to-pitch and run-to-run repeatability were demonstrated experimentally.

A novel swirl simulator was designed and commissioned in the OTRF by Qureshi and Povey [4] to produce a swirling velocity profile based upon extreme exit swirl conditions of a modern lean-burn combustor. Area survey measurements showed that the vortex and peak swirl angles (of over  $\pm 40$  deg) were well matched to the target profile. A high degree of repeatability between runs was also demonstrated.

These combustor simulators enabled several experimental and computational studies of the effects on the turbine heat transfer due to hot-streaks [5–10] and swirl [11–13] individually. For both systems, the mass flow rate and turbine inlet enthalpy were measured to high accuracy (as described by Beard et al. [14]), thus permitting accurate turbine performance measurements. In particular, Beard et al. [15,16] measured mass-averaged efficiency penalties of  $-0.29\%$  and  $-1.19\%$  with hot-streaks and swirl, respectively.

The computational study by Khanal et al. [17] suggests that the effects of swirl and hot-streaks in isolation cannot be superimposed to predict their effects in combination. Nevertheless, to the best of our knowledge, no experimental studies published to date have considered the effects of combined hot-streaks and swirl on the turbine.

Hall et al. [18] reported the first design of a fully annular lean-burn combustor simulator. This simulator, which is the focus of this study, was designed for use in the OTRF using an unsteady Reynolds-averaged Navier–Stokes (URANS) computational fluid dynamics (CFD) approach. Subsequently, the simulator was experimentally characterized using a bespoke blow-down test facility operating at atmospheric conditions [19]. The generated temperature and swirl profiles were well matched to the target data as well as CFD predictions and also showed a high degree of pitch-to-pitch repeatability.

Koupper et al. [20] reported the design of another lean-burn combustor simulator for turbine experiments with temperature distortion and swirl. Characterization experiments conducted using an annular sector facility have since been reported by Bacci et al. [21]. However, no experimental data from the fully annular system have been published to date.

This paper reports the commissioning in the OTRF of the lean-burn combustor simulator developed by Hall et al. [18]. The simulator has been modified with respect to the configuration described in Ref. [18] in accordance with the differing target profiles. Prior to installation in the OTRF, detailed experimental measurements of the new profile were obtained using the aforementioned

atmospheric test facility. These results are presented and compared to the target profile.

## The Oxford Turbine Research Facility

The OTRF is a short-duration wind tunnel capable of matching to engine conditions of the nondimensional parameters relevant to turbine fluid mechanics and heat transfer; namely the Mach number, Reynolds number, corrected speed, gas-to-wall temperature ratio, and turbulence intensity. A schematic of the OTRF is shown in Fig. 1.

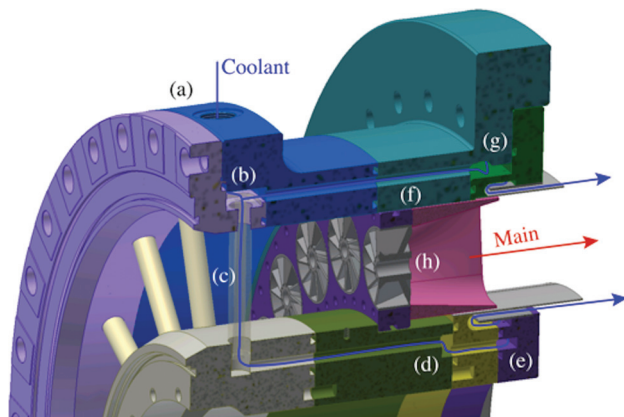
The design and operation of the facility was first described by Hilditch et al. [22]. Prior to a run, the plug valve is closed, the test section is evacuated to approximately 10 mbar and the rotor is spun to the turbine design speed. High-pressure air is injected behind a light free piston driving it down a large piston tube, which compresses the test air (approximately isentropically) to the desired turbine inlet stagnation conditions. The fast-acting plug-valve then opens, allowing the test gas to pass through the working section. The turbine pressure ratio is set by means of an adjustable-area second (normally choked) throat situated downstream of the turbine. Downstream of the second throat, the flow passes through an aerodynamic turbobrake, which is connected to the rotor shaft maintaining a constant rotor speed during the test run. Steady conditions are achieved for approximately 400 ms.

For the present investigation, the facility was fitted with the low-emissions core engine technologies (LEMCOTEC) turbine, a new 1.5-stage research turbine recently designed by Rolls-Royce and GKN that is representative of typical modern engine architectures. The design and commissioning of the LEMCOTEC turbine is reported in Beard et al. [23]. The design operating conditions of the LEMCOTEC turbine in the OTRF are presented in Table 1.

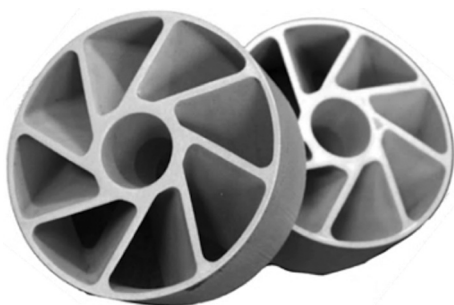
The combustor simulator, which is the focus of this paper, was installed in the OTRF between the plug valve and the turbine stage (see Fig. 1). During a run, the coolant required to generate the OTDF profile is supplied from an air reservoir at ambient temperature and metered using a calibrated sonic venturi with an associated mass flow rate uncertainty of  $\pm 0.57\%$  (to 95% confidence).

Table 1 Operating conditions of the LEMCOTEC turbine in the OTRF

Parameter	Nominal value
$Re_{NGV}$	$2.13 \times 10^6$
$\Gamma = \dot{m} \sqrt{T_{01}} / p_{01}$	$5.897 \times 10^{-4} \text{ kg s}^{-1} \text{ K}^{1/2} \text{ Pa}^{-1}$
$N / \sqrt{T_{01}}$	$385.1 \text{ rpm K}^{-1/2}$
$p_{01} / p_{4, \text{hub}}$	3.555
$T_{01} / T_w$	1.64



**Fig. 2 CAD model of the lean-burn combustor simulator: (a) coolant entry, (b) common coolant plenum, (c) hub feed rod, (d) hub coolant feed, (e) hub injection plenum, (f) case coolant feed, (g) case injection plenum, and (h) mainstream swirler assembly**



**Fig. 3 Photograph of single-piece water jet-cut swirlers**

### Combustor Simulator Operation

The design methodology for the combined hot-streak and swirl profile combustor simulator is described in detail by Hall et al. [18]. The simulator has a modular design enabling the generation of a range of engine-representative swirl and hot-streak profiles thereby facilitating turbine interaction studies with various traverse shapes and swirl intensity. A sectioned CAD model of the combustor simulator is shown in Fig. 2.

The swirl profile in the mainstream flow was generated by discrete swirlers (see Fig. 3) mounted in a flat plate, which have been shown to be effective in producing strong swirl at moderate pressure drop [24]. The swirlers can be interchanged to modify the swirl strength, and axial movement of the mounting plate allows for fine adjustment. The number of swirlers is simply altered by changing the mounting plate. The swirling mainstream flow exits the swirlers into rounded-sector diffusers which delays mixing of adjacent vortices and controls the rate of diffusion from the swirlers into the larger area duct.

Radial temperature nonuniformity is generated by ejecting cold (ambient) gas of a mass flow rate,  $\dot{m}_c$ , from annular slots at the hub and casing end-walls downstream of the swirler plate. Before ejection, the hub and casing coolant streams are preswirled by approximately 20 deg to minimize shear mixing due to the velocity mismatch with the swirling mainstream. The magnitude and shape of the generated radial temperature profile can be altered by changing the total coolant mass flow rate and the mass flux split between the hub and casing feeds.

Nominally uniform turbine inlet conditions can be achieved by setting  $\dot{m}_c = 0$  and replacing the swirler plate with a system of radial rods, which act as passive turbulence generators. The combustor simulator can also be configured to generate a radial

temperature profile only (swirler plate replaced by a system of radial rods and  $\dot{m}_c > 0$ ), or swirl only ( $\dot{m}_c = 0$ ).

### Commissioning of Combustor Simulator Coolant Feed System

The coolant feed system was tuned during commissioning to achieve a particular design hub/casing mass flux ratio. The overall (hub plus case) coolant mass flow rate was metered using an ISO calibrated sonic nozzle (overall measurement uncertainty of  $\pm 0.57$ –95% confidence). The split between the hub and casing feeds was achieved with a system of radial holes in hub and casing feed rings. By operating the system with the holes choked, and by blocking discrete holes at either hub or casing, the mass split between the two systems could be adjusted. The process for doing this is now described.

In an initial experiment, the hub feed holes were blocked, and blowdown experiments (venting to atmosphere) were conducted to determine the discharge coefficient of the choked casing feed holes. The discharge coefficient is calculated as

$$C_d = \frac{\dot{m}_{c,case}}{n_{hole} A_{hole} p_{0c}} \sqrt{\frac{RT_{0c}}{\gamma}} \left(1 + \frac{\gamma - 1}{2}\right)^{\frac{\gamma + 1}{2(\gamma - 1)}} \quad (1)$$

where  $p_{0c}$  and  $T_{0c}$  are the coolant stagnation conditions measured in the casing plenum, and  $\dot{m}_c$  was directly measured using the calibrated sonic venturi.

Subsequently, similar experiments were conducted with both the hub and casing feed holes unblocked, to determine the mass flux ratio and discharge coefficient of the choked hub feed holes (Eq. (1) for the hub feed, with the hub mass flow rate calculated as  $\dot{m}_{c,hub} = \dot{m}_c - \dot{m}_{c,case}$ ). Finally, a subset of individual casing feed holes were blocked until the design hub-to-casing mass flux ratio was achieved (to within  $\pm 1\%$ ).

### The Low-Emissions Core Engine Technologies Target Profile

The simulator design target resulted from an iterative design process (based on URANS simulations), which aimed to achieve conditions representative of a modern lean-burn combustor. In particular, the target profile was required to produce a clockwise vortex with peak swirl angles of  $+33.0$  and  $-25.0$  deg; a strong radial nonuniformity in total temperature; a representative total pressure profile with low total pressure in the vicinity of the vortex core; and high turbulence intensity driven by the vortex structure. At the end of this design process, the final URANS simulation was chosen as the target profile. This design process led to the following design parameters: swirler vane angle 35 deg,  $\dot{m}_h/\dot{m}_c = 3.33$ ,  $\dot{m}_{c,case}/\dot{m}_{c,hub} = 1.13$ . The resulting target profile is shown in Fig. 4 over a single swirler pitch and from hub to casing radially. Indicated are the circumferential positions of the swirlers and the leading edges (LE) of the HP nozzle guide vanes (NGV), although the latter were not featured in the URANS simulations. As is discussed later, the NGVs aligned and misaligned with the swirlers are labeled as S1 and S2, respectively.

The yaw angle,  $\alpha$ , is the angle between the projection of the flow velocity vector onto the meridional plane and the machine axis (defined as positive in the direction away from the machine axis). The pitch angle,  $\beta$ , is the angle between the projection of the velocity vector onto a surface of constant radius and is defined as positive in the direction of shaft rotation. The swirler total pressure loss coefficient,  $\zeta_{Sw}$ , is defined as

$$\zeta_{Sw} = \frac{p_{0,Sw} - p_0}{q_{Sw}} \quad (2)$$

where  $p_0$  is the local total pressure at the plane of interest,  $p_{0,Sw}$  is the total pressure upstream of the swirler, and  $q_{Sw}$  is the dynamic pressure through the swirler, defined as



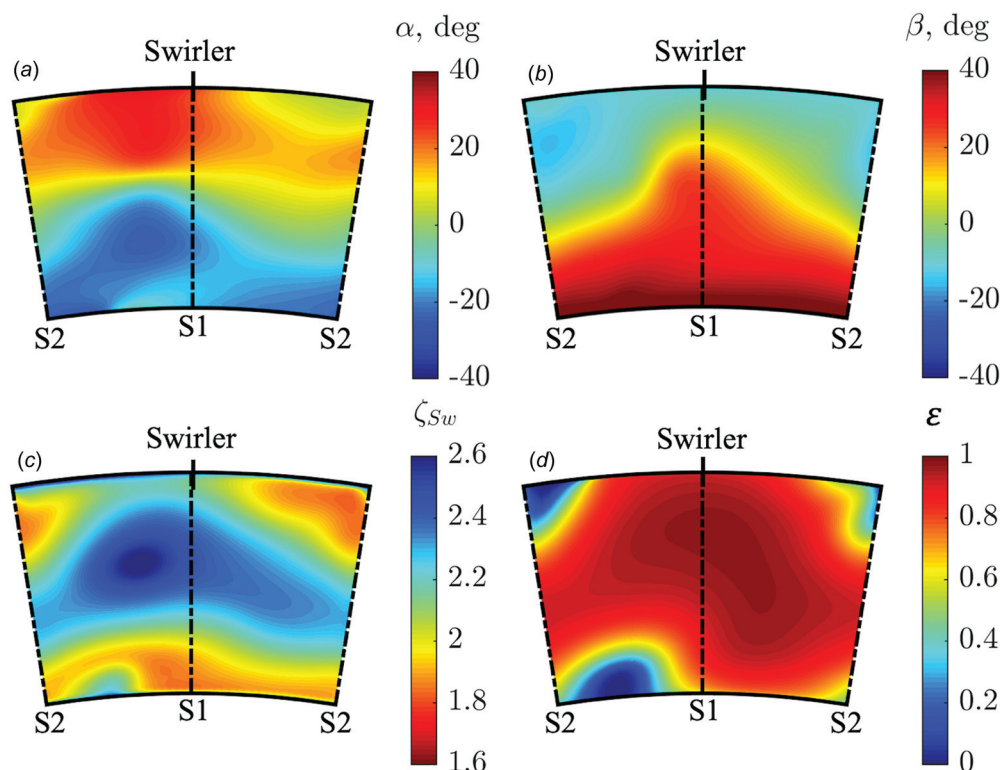


**Fig. 4 Predicted combustor simulator exit profiles at OTRF conditions: (a) yaw angle, (b) pitch angle, (c) swirler total pressure loss coefficient, and (d) total temperature effectiveness. The swirler centerline is aligned with the center of the profile. Viewing orientation is from downstream.**

$$q_{Sw} = \frac{\dot{m}_h^2}{2\rho_{Sw}A_{Sw}^2} \quad (3)$$

where  $A_{Sw} = \pi r_{Sw}^2$  is a planar area based on the outer radius of the swirler passage,  $r_{Sw}$ . The total temperature effectiveness,  $T_{0,eff}$ , is defined as follows:

$$T_{0,eff} = \frac{T_0 - T_{0c}}{T_{0h} - T_{0c}} \quad (4)$$

where  $T_0$  is the local total temperature at the plane of interest, and  $T_{0h}$  is the coolant total temperature.

The yaw and pitch angle profiles show a well-defined vortex core, whose position is offset from the geometric swirler center by approximately +3 deg in the pitchwise direction. This migration of the vortex is consistent with the net swirl around the annulus imparted by the individual swirler cores (note that the net swirl velocity goes down significantly based on the machine axis due to the large radius). The  $\zeta_{Sw}$  profile shows low total pressure associated with the vortex core and high total pressure near the endwalls due to cold gas ejection. The  $T_{0,eff}$  profile shows strong radial and weak circumferential nonuniformities. Overall, the target profiles (defined by the last URANS prediction in the iterative design process) can be considered to be typical of a lean-burn combustor exit flow.

### Atmospheric Test Facility

Obtaining detailed area surveys of the flow at turbine inlet in the OTRF is made challenging by the limited probe access and the short test duration nature of the facility. To allow a high-resolution survey of the simulator exit flow, a bespoke experimental facility was developed. The design and operation of the

facility, shown schematically in Fig. 5, was described in detail by Hall and Povey [19]. The facility was a regulated blow-down tunnel (run duration  $\sim 30$  s) which exhausted to atmosphere through a representative turbine inlet contraction, but without NGVs. (Previous measurements conducted downstream of a swirl simulator operating in an atmospheric test facility with NGVs absent showed only small changes compared to measurements conducted in the OTRF with the NGVs present [4].) The atmospheric test facility was designed for 360-deg traverse capability, to allow detailed experimental surveys of the combustor simulator exit flow.

The same hardware as used in the OTRF was tested in this atmospheric test facility. Mainstream gas was supplied at ambient temperature and constant pressure (via a gas regulator) from a large pressure vessel. The stagnation conditions of the mainstream flow were measured upstream of the swirlers using pitot and thermocouple rakes. Cold air was supplied at approximately 275 K from a large Ranque-Hilsch vortex tube. The cold stream stagnation conditions were measured in hub and casing plenums using circumferentially distributed thermocouple and pitot probes. The resulting temperature differential between the hot and cold streams was approximately 15 K. Although the temperature differential was considerably lower than in the OTRF, it was sufficient for a nondimensional temperature profile to be defined from measurements. The operating conditions of the atmospheric test facility are compared to those of the OTRF in Table 2.

An intrinsic limitation of the atmospheric test facility was that it was impossible to match all the correct nondimensional conditions of the OTRF. The most important nondimensional parameter, the swirl number, was matched, however, by virtue of its dependence only on the swirler geometry (which is identical in both facilities). Because of the comparatively low operating pressure and temperature of the atmospheric test facility, the Reynolds number was lower than in the OTRF (by almost an order of

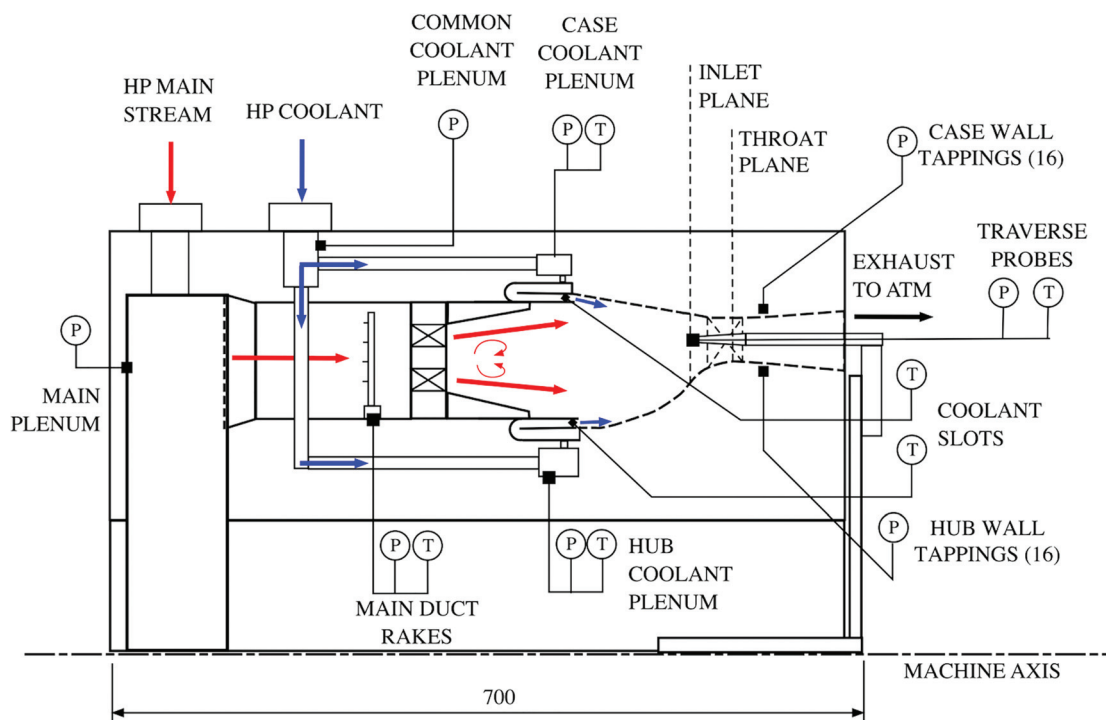


Fig. 5 Sectional schematic of the combustor simulator test facility developed by Hall et al. [19]. Instrumentation points and NGV locations are indicated.

Table 2 Summary of combustor simulator operating conditions at design point in the atmospheric test facility and the OTRF

Parameter	Atmospheric test facility	OTRF
$p_0$ (bar)	1.0	8.5
$T_{0h}$ (K)	285	530
$T_{0c}$ (K)	275	290
$T_{01}$ (K)	283	475
$\dot{m}_h$ (kg s <sup>-1</sup> )	2.700	17.690
$\dot{m}_c$ (kg s <sup>-1</sup> )	0.300	5.310
$Re_{Sw}$	$1.1 \times 10^5$	$7.3 \times 10^5$

magnitude). In general, in separated flows of the type that dominate the combustor simulator, the Reynolds number could be considered to be relatively unimportant. It is known, however, to potentially influence the vortex breakdown/stability modes [25], and must therefore be checked carefully in CFD studies at both the representative condition and the lower Re condition. This check was performed, and the flows were found to be similar in structure and in terms of the nondimensional loss (see discussion in the following section, Computational Study of the Combustor Simulator). The flows are incompressible, and therefore, Mach number effects were not considered significant.

### Computational Study of the Combustor Simulator

As discussed previously, the target combustor simulator exit flow field was defined using an iterative CFD design process described by Hall et al. [18]. The URANS simulations both at the test conditions of the atmospheric test facility and at OTRF conditions are now described, in order to verify that the vortex breakdown/stability modes were consistent at both conditions.

**Numerical Setup.** Unsteady Reynolds-averaged Navier–Stokes simulations were conducted using ANSYS FLUENT with second-order

spatial and temporal discretization, SIMPLE pressure–density coupling, the Reynolds stress model for turbulence closure, and a time-step of  $10^{-5}$  s. A multiblock hexahedral mesh comprising  $2.8 \times 10^6$  cells was used to model a domain from upstream of the hub coolant feed rods to the axial location corresponding to the LEMCOTEC NGV trailing edge (TE)—see Fig. 6. Standard wall functions were used at the near-wall regions. Time-resolved simulations were run until periodic flow was established, which typically required 100 ms of flow time or approximately five flow-through periods of the volume from swirler inlet to domain exit.

**Predictions at Atmospheric Test Facility Conditions and at Oxford Turbine Research Facility Conditions.** Figure 6 shows time-resolved results from the URANS simulations of the combustor simulator at atmospheric test facility and OTRF conditions. Flow visualizations are shown in order to demonstrate the high degree of similarity between the flow structures and profiles predicted by the two simulations. For both simulations, form of the central recirculation zones (CRZ) indicated by isosurfaces of static pressure, and axial velocity contours,  $u_x$ , shown on the meridional plane through the center of the swirler, are largely indistinguishable. Area contours of  $T_{0,eff}$  and  $\alpha$  at the turbine inlet plane (whose axial position is indicated in Fig. 4) also show a high degree of similarity to one another.

For both simulations, the shape of the CRZ was fairly steady. Crucially, the vortex around the CRZ did not exhibit low-frequency unsteadiness (typically 1–2 kHz) associated with a precessing vortex core or other vortex breakdown modes that have been shown to form for other nonreacting swirl simulator configurations [18].

The similarity in URANS results at both conditions is in agreement with the experimental results reported by Qureshi and Povey [4], who measured similar yaw and pitch angle profiles during a pilot study of a similar swirl generator at atmospheric conditions and during so-called “push-through” experiments in the OTRF (with slightly elongated run times facilitating area survey measurements).

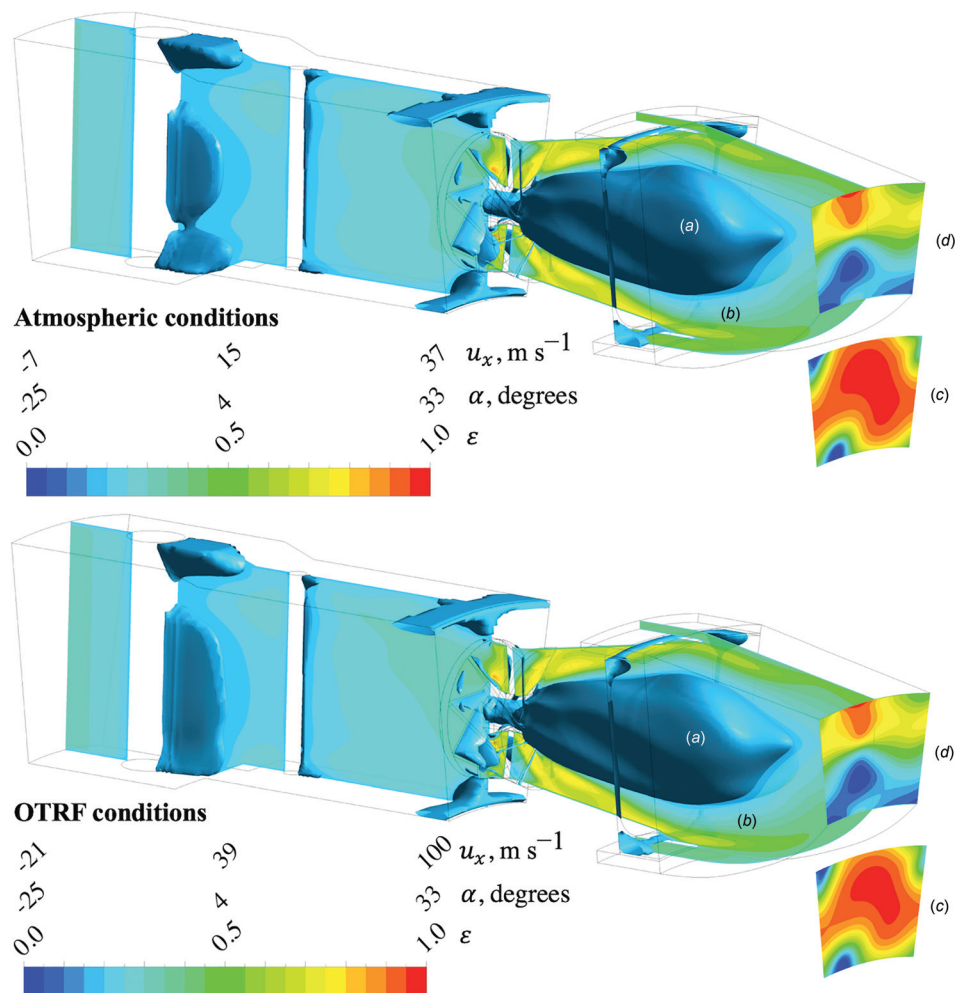


**Fig. 6 Time-instantaneous URANS predictions of the combustor simulator at atmospheric test facility (above) and OTRF conditions (below): (a) central recirculation zone, (b) axial velocity on meridional plane, (c)  $T_{0,eff}$  at turbine inlet plane, and (d) yaw angle at turbine inlet plane**

### Experimental Characterisation at Atmospheric Conditions

High spatial resolution area traverse measurements were conducted to characterize the combustor simulator exit flow-field. A two-axis traverse system was used to conduct area surveys over a circumferential range of  $\pm 27$  deg (3 swirler pitches) to gauge consistency of the flow field across several vortex cores.

A five-hole probe was used to survey the flow angle (yaw and pitch) and total pressure profiles while thermocouple probes ( $k$ -type  $50\text{ }\mu\text{m}$  bare-bead) were used to survey the total temperature profile. The five-hole probe was calibrated over a range of  $\pm 40$  deg in both yaw and pitch angle in the Oxford Probe Calibration Facility, described in detail by Hall and Povey [26].

Five-hole probe traverses were conducted with a minimum of 16 radial increments (spacing of  $\sim 1$  mm) over a range from 19% to 91% radial span (closer proximity to the endwalls was made impossible by the probe size and annulus-line shape). Thermocouple probe traverses were conducted with a minimum of 27 radial increments between 2% and 99% radial span. For this purpose, two thermocouple probes were used, of which one was bent (goose-necked) in order to obtain the measurements close to the endwalls.

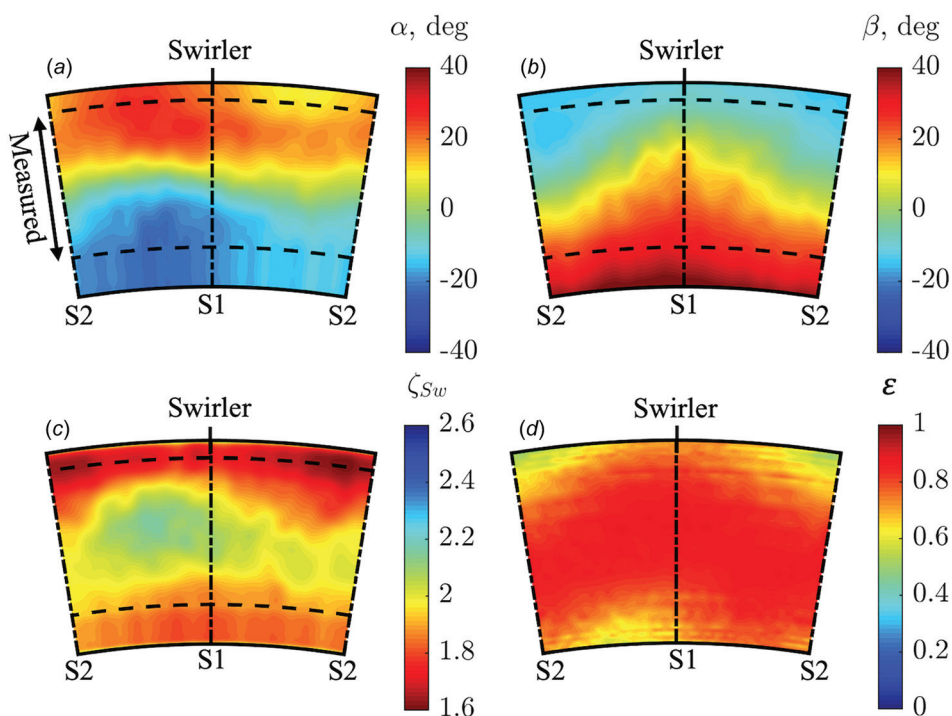
The five-hole probe traverse speed (7.2 deg per second) was chosen to permit high circumferential measurement resolution (at least 225 points per swirler pitch at each radial height) based on the experimentally determined frequency response of the probe

( $-3$  dB cutoff frequency of at least 90 Hz). The lower frequency response of the thermocouple probe (10 Hz) resulted in lower circumferential resolution (25 points per swirler pitch at each radial height) in the total temperature survey data. For this type of probe and calibration procedure, typical uncertainties associated with the measurements of flow angle, total pressure loss coefficient, and total temperature are  $\pm 0.2$  deg,  $\pm 0.5\%$ , and  $\pm 0.4\%$ , respectively. Figure 7 shows the two-dimensional (2D) profiles measured in the atmospheric test facility.

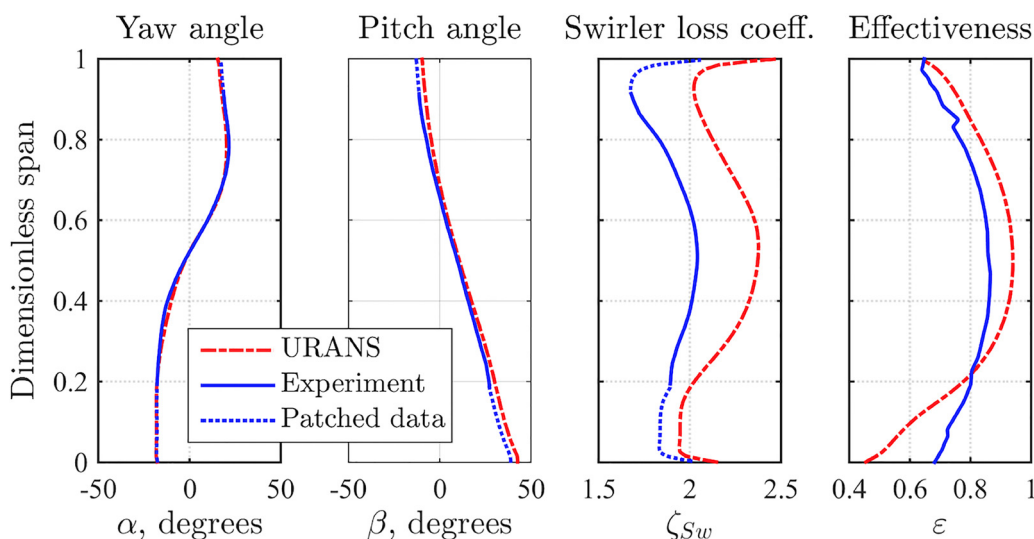
The data in Fig. 7 were acquired at the turbine inlet plane (whose axial position is indicated in Fig. 4). The dashed circumferential lines indicate the radial limits of the area surveys. Data radially outside of the measured region have been extrapolated using radial trends from URANS predictions (circumferentially averaged) fixed to the local measured values at a particular circumferential location at the radial limit of the measured region. Excellent consistency was shown across the three swirler pitches that were surveyed, and therefore, the results are shown for only a single swirler pitch.

Figure 8 presents radial profiles obtained by circumferentially averaging the predicted and measured data presented in Figs. 4 and 7, respectively. In terms of flow angles, the experimental measurements show very good agreement with the target. In particular, a well-defined vortex core is observed approximately  $+3$  deg offset from the swirler centerline in the pitchwise direction (which is consistent with the net swirl around the annulus imparted by the individual swirler cores). The peak measured





**Fig. 7 Combustor simulator exit profiles measured in the atmospheric test facility: (a) yaw angle, (b) pitch angle, (c) total pressure loss coefficient, and (d) total temperature effectiveness. All contours are plotted as viewed from downstream.**



**Fig. 8 Circumferentially averaged combustor simulator exit profiles of yaw angle, pitch angle, total pressure loss coefficient and total temperature effectiveness**

swirl angles of +30.9 deg and −28.4 deg compare reasonably well to the peak swirl angles in the target profile (+33.0 deg and −25.0 deg). The measured radial profiles of yaw and pitch angle show excellent agreement with the target.

The measured loss profile  $\zeta_{Sw}$  agrees well in general form with the target profile but differs significantly in magnitude: there is a well-defined loss core (central peak) with elevated total pressure near the endwalls. There is significant over-prediction of loss by the URANS calculation, which may result from the turbulence model used (the flow is complex, in that it is separated and partially recirculating, with loss dominated by activity in free shear layers). The poor agreement in absolute values is of limited practical significance because when scaled to OTRF conditions (an

environment in which the dynamic pressure to total pressure ratio is very low), the resulting proportional total pressure drop and degree of nonuniformity are both relatively small. Scaling is accounted for in the analysis that follows.

The experimentally measured  $T_{0,eff}$  profile is dictated by coolant migration and mixing and features a strong circumferentially averaged (radial) profile compared to the radially averaged (circumferential) profile (not shown). This is typical of lean-burn combustors. While there is good agreement with the target profile across most of the span, there is significant disagreement below 20% radial span. In both the measured and predicted  $T_{0,eff}$  profiles, migration of hot gas toward the endwalls is observed, despite preswirling of the cold gas before ejection (without this

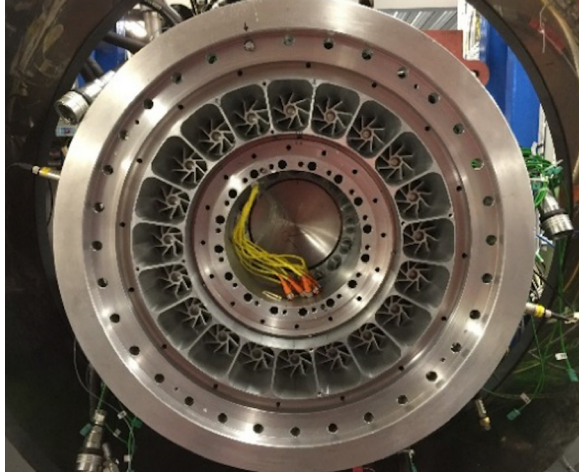


**Fig. 9 Lean-burn combustor simulator installed in the OTRF**

preswirling, greater mixing between the hot and cold streams might be expected due to the more aggressive shear layer that would result).

The experimental results from the atmospheric test facility demonstrated that the system had the ability to produce a flow field representative of a lean burn combustor. There was good agreement between the URANS predictions and experiment for flow angles across the turbine inlet plane and for the general form of the total pressure and temperature profiles. Absolute values for the pressure and temperature profiles were less well reproduced.

### Commissioning in the Oxford Turbine Research Facility

After experimental validation in the atmospheric test facility, the combustor simulator was installed and commissioned in the OTRF. The objective of commissioning was to verify both that the correct mass flow rates and stagnation conditions were achieved during a sufficient period of the relatively short run, and also that the  $T_{0,eff}$  profile was well matched to the target. It was assumed that the swirl profile measured in the atmospheric test facility would be representative of that in the OTRF.

Figure 9 shows a photograph of the combustor simulator installed in the OTRF taken from downstream with the working section removed. The 20 discrete swirlers are visible within the diffusers.

Determining the mass-mean total temperature at stage inlet requires measurements of the mass flow rates and total temperatures of the hot and cold streams supplied from the combustor simulator. Because the OTRF is a transient facility, convective heat transfer must be considered. In the OTRF, the combustor simulator cold stream is delivered to the hub and casing ejection slots at ambient temperature. Because the cold stream supply feeds are also at ambient temperature during a run, convective heat transfer to/from the cold stream between the measurement point and the ejection slots is negligible. However, due to the large temperature difference (approximately 240 K) between the hot stream and the combustor simulator components, significant convective heat transfer to the combustor simulator components (in particular to the swirlers) can be expected to reduce the temperature of the hot stream.

To determine the accurate hot stream total temperature (which permits calculation of the mass-mean total temperature) at turbine inlet, the hot stream temperature drop across the combustor simulator must be accounted for. This was achieved by measuring the swirler-upstream temperature,  $T_{0Sw}$ , and applying a correction to obtain the swirler-downstream total temperature,  $T_{0h}$ .

By combining the steady flow energy equation and the convective heat transfer equation, it can be shown that

$$\Theta = \frac{T_{01} - T_{0Sw}}{T_w - T_{0Sw}} = \frac{hA_w}{\dot{m}_h c_p} \quad (5)$$

where  $\Theta$  is a dimensionless swirler total temperature drop that normalizes the hot stream total temperature drop by the gas-to-wall temperature difference,  $A_w$  is the wetted area of the combustor simulator hardware between the upstream and downstream measurement points, and  $h$  is the average convective heat transfer coefficient over  $A_w$ . For a fixed swirler geometry,  $h$  and  $\dot{m}_h$  are both functions of the swirler Reynolds number,  $Re_{Sw}$ , based on the outer diameter of the swirler passage,  $d_{Sw} = 2r_{Sw}$ . Therefore,  $h/\dot{m}_h$  is also a function of  $Re_{Sw}$  and we can write

$$\Theta = f(Re_{Sw}) \quad (6)$$

It is noted that  $h$  is also a function of the Prandtl number,  $Pr = \mu c_p / k$ , where  $\mu$ ,  $c_p$ , and  $k$  are the dynamic viscosity, specific heat capacity, and thermal conductivity of the gas, respectively. However, since for air,  $Pr$  is only a weak function of temperature, and the temperature differences between commissioning tests were relatively small, we neglect  $Pr$  effects from this analysis.

To determine the appropriate correction, experiments were conducted to measure the transient temperature drop across the combustor simulator. To prevent the effects of partial mixing with the cold stream, only the hot stream was supplied during these tests. The hot stream mass flow rate was measured using the piston tube exit contraction as a subsonic venturi (as was also done during normal OTRF testing). This measurement system, including the calibration of the contraction, was described by Beard et al. [14]. The bias and precision uncertainties associated with the hot stream mass flow rate measurement system were  $\pm 1.29\%$  and  $\pm 0.159\%$  (to 95% confidence), respectively.

Without the cold stream flowing, the mass-mean total temperature at turbine inlet was increased as the hot stream temperature was unchanged. Because the inlet total pressure and the capacity of the near-choked NGV were unchanged (to first order), the turbine mass flow rate was reduced. However, the swirler mass flow rate,  $\dot{m}_h$ , was increased as it now occupied the all of the NGV capacity. Expressing  $Re_{Sw}$  as

$$Re_{Sw} = \frac{\dot{m}_h d_{Sw}}{\mu A_{Sw}} \quad (7)$$

shows that an increase in  $\dot{m}_h$  causes a proportional increase in  $Re_{Sw}$  and can thus be expected to alter the heat transfer characteristics (and hence  $\Theta$ ). Note that because the hot stream temperature was unchanged, so also was the viscosity,  $\mu$ , in Eq. (7). In order to match  $Re_{Sw}$  (and therefore  $\dot{m}_h$ ) during the temperature drop characterization experiments to the conditions achieved during normal testing, the turbine inlet total pressure,  $p_{01}$  (and hence  $p_{0Sw}$ , which was greater to account for loss across the swirler) was scaled by  $\dot{m}_h/\dot{m}'_h$ , where  $\dot{m}'_h$  is the new (increased) swirler mass flow rate for tests without the combustor simulator cold stream flowing. Accordingly, experiments were conducted at the reduced total pressure of  $p_{0Sw} = 6.79$  bar.

Figure 10 shows the measured  $Re_{Sw}$  plotted against  $\dot{m}_h$ , where both quantities have been time-averaged over the aerodynamically stable period of each run. The data collapse onto a linear fit ( $r^2 > 0.99$ ), as was expected due to the proportionality of  $Re_{Sw}$  and  $\dot{m}_h$  discussed previously. Furthermore, the data lie close to the design condition (indicated by a red cross marker), at which normal testing was conducted.

The total temperature drop across the combustor simulator was measured using six thermocouples installed upstream of the simulator and 13 thermocouples installed at the turbine inlet plane. The thermocouples were k-type 25  $\mu\text{m}$  bare beads. The upstream thermocouples agreed to within  $\pm 1$  K or 2.8% of the measured



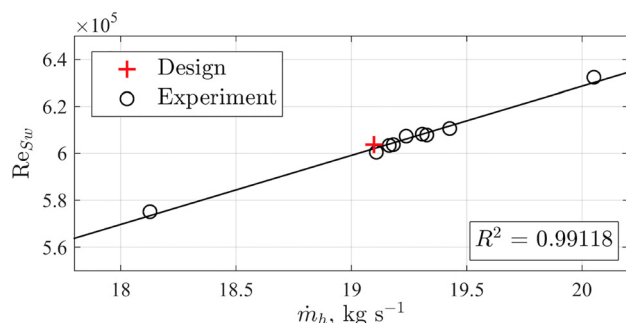


**Fig. 10 Time-averaged  $Re_{Sw}$  versus  $\dot{m}_h$  for the nine OTRF experiments conducted to measure the hot stream total temperature drop across the combustor simulator. The design condition is also indicated for reference.**

temperature drop (36.2 K, discussed later), indicating a high degree of temperature uniformity. The downstream thermocouples were distributed over a range of radial and circumferential positions with respect to the swirlers and the results indicated peak-to-peak variation  $\pm 7$  K (19% of the temperature drop) and standard deviation  $\pm 2$  K (5.5% of the temperature drop). Upstream and downstream measurements were averaged over all thermocouples at each station before their difference was calculated. The wall (metal) temperature was measured prior to the start of each run. This was assumed temporally constant given the short duration of the test ( $\sim 0.5$  s) compared to the time-constant of the simulator hardware (order of minutes) due to the low Biot number of the system. This assumption was verified using wall temperature measurements elsewhere in the facility.

Figure 11 shows the measured nondimensional hot stream total temperature drop,  $\Theta$ , across the combustor simulator in the OTRF as a function of time. The trace is averaged over nine synchronized test runs and the standard deviation between these runs is indicated. The trace is reasonably stable during the steady period of the run at a time-mean value of  $\Theta = 0.151$ . At the design conditions  $T_w = 290$  K and  $T_{0Sw} = 530$  K, this corresponds to a hot stream total temperature drop of 36.2 K (6.8% of the upstream temperature) while the transient standard deviation remains within  $\pm 4.7$  K (0.9% of the upstream temperature). As a result, the  $T_{0Sw}$  target value was not increased to account for the hot stream temperature drop across the swirlers and so the achieved mass-mean total temperature at turbine inlet, given by

$$\bar{T}_{01} = \frac{\dot{m}_h T_{0h} + \dot{m}_c T_{0c}}{\dot{m}_h + \dot{m}_c} \quad (8)$$

was 446.4 K, which is 28.6 K or 6.0% below the design value of 475 K.

During normal testing,  $\bar{T}_{01}$  was determined as follows. First,  $T_{0h}$  was calculated via Eq. (5) using measurements of  $T_{0Sw}$ ,  $T_{0c}$ , and  $T_w$ , and  $\Theta$  set equal to the time-mean of the run-averaged trace shown in Fig. 11. The resulting  $T_{0h}$  trace was then combined with measurements of  $\dot{m}_h$ ,  $\dot{m}_c$ , and  $T_{0c}$  according to Eq. (8). The remaining parameters required to determine the turbine operating condition were measured as described in the following section, Measurement of Mass-Mean Operating Condition.

**Measurement of Mass-Mean Operating Condition.** Measured traces of the turbine inlet conditions for a typical OTRF run with the combustor simulator installed are shown in Fig. 12. The vertical dashed lines indicate the steady test period. The total pressure upstream of the combustor simulator,  $p_{0Sw}$ , is the average of four pitot measurements. The turbine inlet total pressure,  $p_{01}$ , is calculated using Eq. (2), with a mass-mean swirler total pressure loss coefficient of 2.06% based on the data shown in Fig. 7(c) scaled to OTRF conditions. The total pressure is stable during the test period (with  $\pm 1\%$  oscillation due to the piston oscillation) and

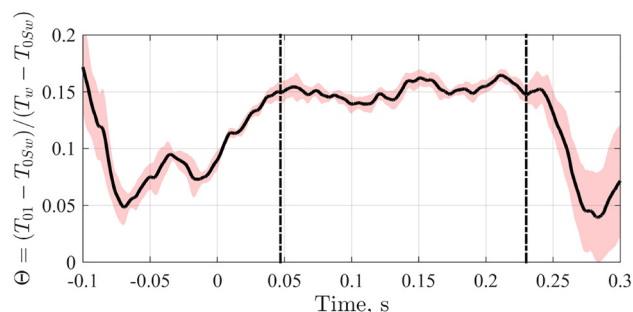


**Fig. 11 Measured transient hot stream nondimensional total temperature drop across the combustor simulator in the OTRF. The standard deviation between nine runs overlaid. Vertical lines indicate the steady period of the run.**

well matched to design value of  $p_{01} = 8.5$  bar. The combustor simulator coolant stream pressure,  $p_{0c}$ , measured in the common coolant plenum (Fig. 2) is also steady during the useful period of the run. The initial transient in  $p_{0c}$  is a result of high-pressure gas stored in the pipework venting after the valve opening. This transient has dissipated before the start of the test period.

The hot stream total temperature,  $T_{0h}$ , is calculated using the method described in the previous section, Commissioning on the Oxford Turbine Research Facility (based on the data shown in Fig. 11). The total temperature upstream of the combustor simulator,  $T_{0Sw}$ , is calculated as the time-average of five thermocouple measurements. The cold stream total temperature,  $T_{0c}$ , is measured using four thermocouples ( $k$ -type 75  $\mu$ m bare bead) distributed around the case injection plenum. These measurements were shown experimentally to agree with measurements in the hub injection plenum. The resulting mass-mean total temperature at the turbine inlet plane is computed using Eq. (8). As desired, all total temperature traces are approximately constant during the steady period of the test (based on pressure).

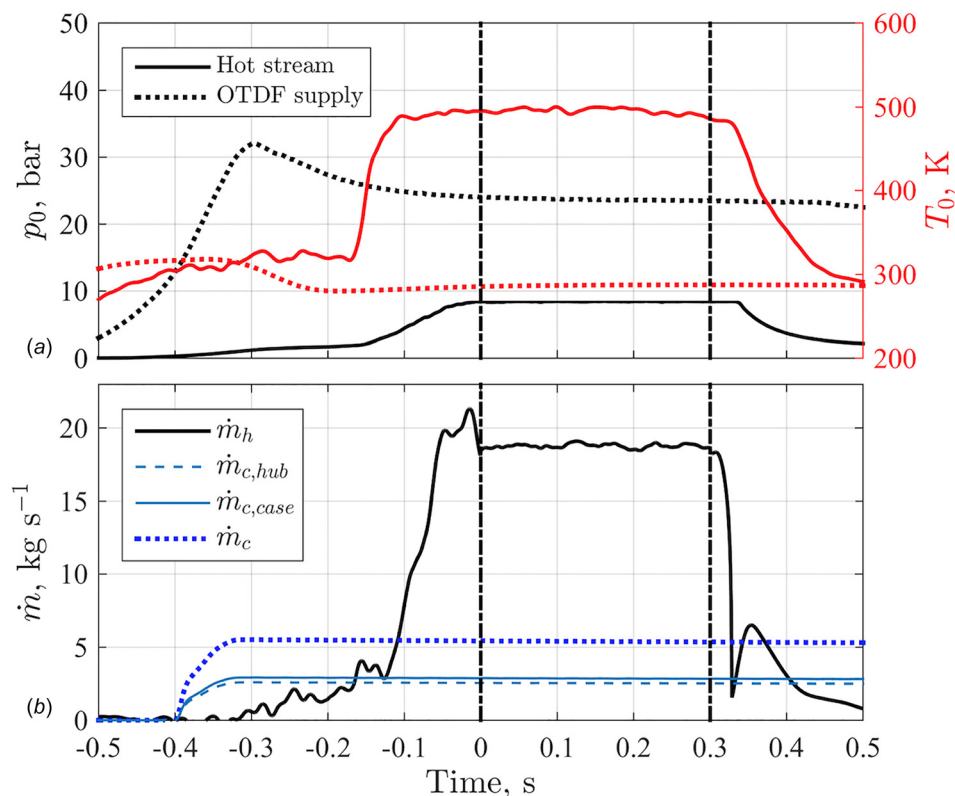
The hot stream mass flow rate,  $\dot{m}_h$ , trace shows small oscillations associated with piston motion. For all mass flows, unsteady corrections as discussed in Ref. [14] were used to account for the change in stored mass within the various plenums between the measurement location and stage inlet. The corrections were found to be insignificant during the runs. The total cold stream mass flow rate,  $\dot{m}_c$ , is metered by a choked venturi nozzle, calibrated to International Organization for Standardization (ISO) standards, prior to entering the combustor simulator. The mass flux split between the hub and casing feed was tuned and measured during commissioning. Notwithstanding piston oscillations, the mass flow rates are all reasonably constant during the runs, as desired.

Table 3 lists the time-mean operating conditions of the combustor simulator in the OTRF, averaged over 20 runs, along with the standard deviation between runs and the overall measurement uncertainties. The average values for all measurements are close to the design values listed in Table 2, except for  $T_{01h}$  and therefore  $\bar{T}_{01}$ , which are lower than design intent due to the convective heat transfer from the hot stream to the simulator hardware. The standard deviations of the data on a run-by-run basis are less than 1% for all direct measurements other than  $\dot{m}_h$ , indicating the high degree of consistency between runs.

The total mass flow rate,  $\dot{m}_h + \dot{m}_c = 24.440$  kg s $^{-1}$ , exceeds the through-flow design value of 23.000 kg s $^{-1}$  by +6.24%. A similar discrepancy (+5.29%) was measured with uniform inlet conditions, suggesting the geometric throat area of the manufactured NGVs is greater than the design intent.

### Stage Inlet Survey Measurements

Area survey measurements of total temperature were conducted to characterize the performance of the simulator at OTRF conditions. The swirl profile was not surveyed in the OTRF because the limited probe access and short test duration give rise to low spatial



**Fig. 12 Stage inlet operating conditions for a typical OTRF run with the combustor simulator installed: (a) total pressure and temperature data and (b) mass flow rate data**

**Table 3 Summary of combustor simulator operating conditions measured during commissioning in the OTRF**

Parameter	Mean (20 runs)	Diff. from design value (%)	Standard deviation (%) (20 runs)	Measurement uncertainty, % (to 95% confidence)
$p_{0sw}$ (bar)	8.676	n/a	$\pm 0.62$	$\pm 0.10$
$p_{01}$ (bar)	8.495	-0.06	$\pm 0.59$	$\pm 0.11$
$T_{0sw}$ (K)	527.2	n/a	$\pm 0.85$	$\pm 0.27$
$T_{0h}$ (K)	491.0	-7.36	$\pm 0.92$	$\pm 0.28$
$T_{0c}$ (K)	286.4	-1.24	$\pm 0.52$	$\pm 0.46$
$T_{01}$ (K)	446.4	-6.02	$\pm 1.35$	$\pm 0.38$
$\dot{m}_h$ (kg s <sup>-1</sup> )	19.097	-0.02	$\pm 1.89$	$\pm 1.30$
$\dot{m}_{c,hub}$ (kg s <sup>-1</sup> )	2.509	+0.53	$\pm 0.60$	$\pm 1.39$
$\dot{m}_{c,case}$ (kg s <sup>-1</sup> )	2.829	+0.53	$\pm 0.18$	$\pm 0.80$
$\dot{m}_c$ (kg s <sup>-1</sup> )	5.338	+0.53	$\pm 0.36$	$\pm 0.57$

resolution and unacceptably high measurement uncertainty (see discussion in Ref. [4]). Because no direct experimental data from the OTRF were available, the assumed swirl profile was based on the swirl profile measured in the atmospheric test facility (extended to the endwalls using the URANS predictions as described previously). This approach was partially justified by the findings of Qureshi and Povey [4], who showed that for a similar swirl generator, there was no significant difference between the profiles obtained via high-resolution atmospheric measurements and low-resolution OTRF measurements. Therefore, there was a high degree of confidence in the measured swirl profile already obtained.

An additional benefit of surveying the  $T_{0,eff}$  profile in the OTRF was that the results could be used as an indicator for any change—though not predicted—in flow structure (such as vortex core destabilization), should it occur in the OTRF.

**Survey Instrumentation.** In the OTRF, there are small temporal variations in the turbine inlet flow-field (periodic total pressure and total temperature fluctuations) arising from piston oscillations.

This makes the use of traverse probes more difficult. For this reason, area-surveys were conducted by sequentially moving (in both radial and circumferential directions) radially arranged rakes over a number of tests. These radial rakes were mounted in one of nine removable minicassettes, each with two radial and three circumferential mounting locations for rakes. Using this scheme, a full area-survey was built up, comprising 27-by-18 (486 measurement locations) measurement points distributed over two NGV pitches (or one swirler pitch).

Area surveys of the total temperature at the turbine inlet were conducted using three radial rakes each featuring nine thermocouples ( $k$ -type 25.4  $\mu$ m bare bead). At turbine inlet design conditions, the time period required to settle to within 0.1% of a given temperature step (in time) was predicted to be approximately 15 ms or less than 4% of the test period. A photograph of the rakes installed in the OTRF is shown in Fig. 13.

**Survey Results.** The OTRF area-survey results of total temperature measured at the stage inlet with the combustor simulator

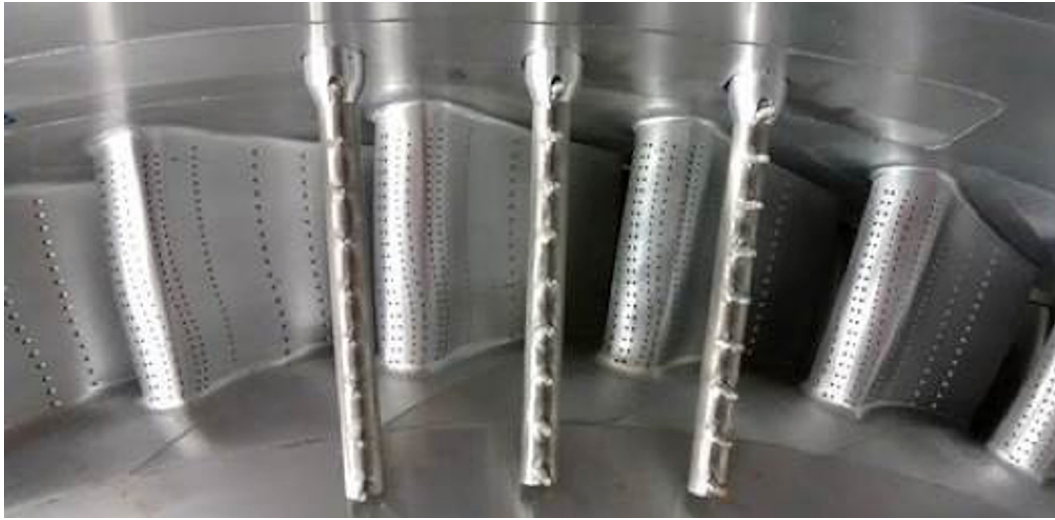


Fig. 13 Photograph of the turbine inlet survey thermocouple rakes installed in the OTRF

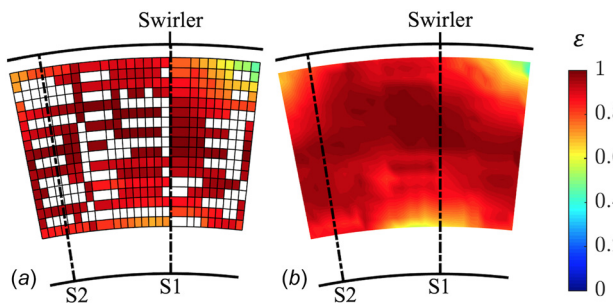


Fig. 14 OTRF stage inlet  $T_{0,eff}$  survey measurements with combustor simulator: (a) area-survey data and (b) interpolated data. Contours are plotted as viewed from downstream.

installed are shown in Fig. 14(a). Data are presented as dimensionless  $T_{0,eff}$  in order to account for small variations in hot and cold stream temperatures between runs. Missing data represent measurement points with a damaged thermocouple and the radial dashed lines indicate NGV LE positions.

To populate the regions where data are missing in the combined survey, values were interpolated using a piecewise cubic Hermite

polynomial. The resulting interpolated profile is also shown in Fig. 14(b).

Due to the rapid contraction of the turbine inlet duct with axial distance (especially the hub annulus line) and the geometry of the radial rakes, the area-survey data covered a range of approximately 20–95% radial span. To help interpret turbine performance measurements it is necessary to have complete inlet boundary conditions (for CFD simulations). An extrapolation technique used to estimate the profile in the missing regions is discussed in the next section, Integration and Scaling of Data Sets.

Figure 15 shows the so-called “patched” (extrapolated)  $T_{0,eff}$  profile. Also shown is a comparison between the radial profile obtained by circumferentially averaging the OTRF measurements and associated patched profile, and those obtained from measurements and predictions from the atmospheric test facility. The OTRF measurements closely match the URANS predictions below approximately midspan. Above midspan, the measurements appear increased by a roughly constant offset, while the shape of the profiles otherwise agree well. Overall, the OTRF measurements compare better with the URANS predictions than with the atmospheric test results.

### Integration and Scaling of Data Sets

This section discusses the integration of experimental data from two test facilities (the atmospheric test facility and the OTRF) and

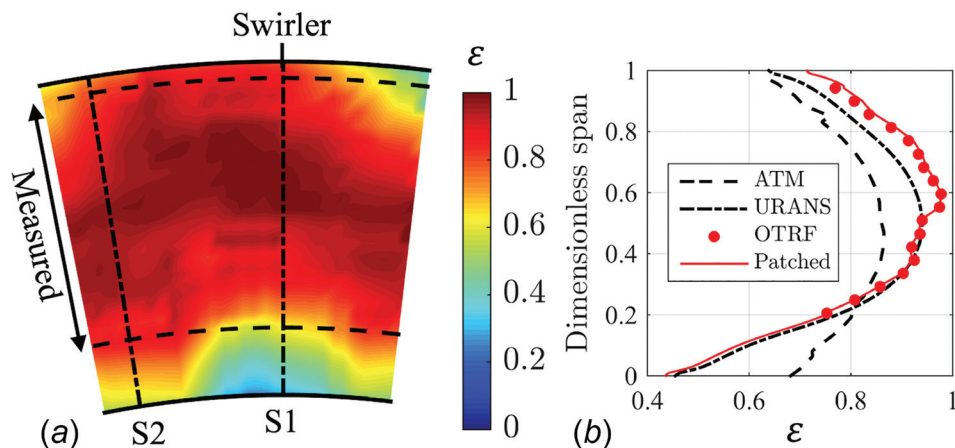
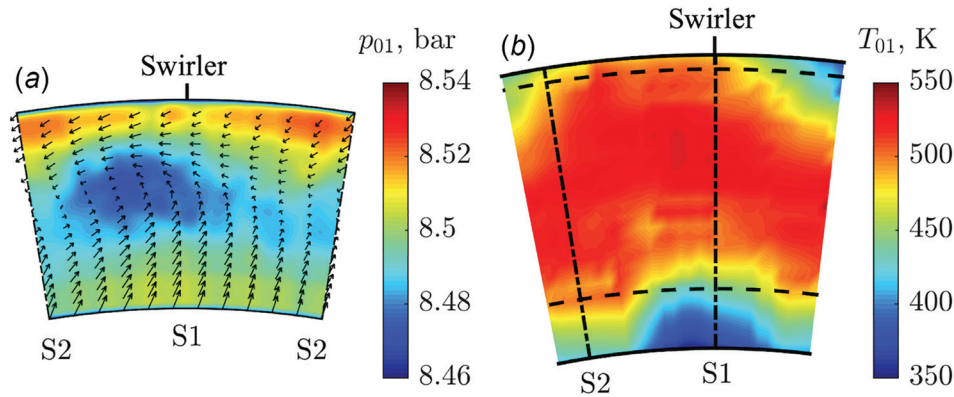


Fig. 15 Full-span stage inlet  $T_{0,eff}$  profiles: (a) measured area-survey data with extrapolation to the endwalls and (b) radial distributions of circumferentially area-averaged profiles





**Fig. 16 Nonuniform inlet boundary conditions imposed in the 1.5-stage CFD model: (a) total pressure contours and secondary velocity vectors and (b) total temperature contours**

computational data from URANS predictions of the combustor simulator. The integrated data are used to generate a suitable 2D boundary condition for CFD validation of the 1.5-stage LEMCOTEC turbine experimental test data.

**Extrapolation of Temperature Data to Generate Full-Span Profiles.** In order to use the measured nonuniform  $T_{0,\text{eff}}$  survey data from the OTRF to prescribe an inlet boundary condition for CFD simulations of the turbine for validation, the data shown in Fig. 14 required extrapolation to the endwalls. This was achieved using a method similar to that used to extrapolate the profiles measured in the atmospheric test facility: circumferentially averaged URANS predictions were fixed to local measured values at each circumferential location. The resulting full-span  $T_{0,\text{eff}}$  profile is shown in Fig. 15. In future OTRF test campaigns, it would be desirable to extend the measurement region radially, so that errors due to extrapolation near the endwalls are avoided.

**Scaling of Nondimensional Profiles to OTRF Conditions.** The dimensionless swirler total pressure loss coefficient profile shown in Fig. 7 can be used to calculate the turbine inlet total pressure profile,  $p_{01}$ , in the OTRF. This is achieved by rearranging Eq. (2) and utilizing Eq. (3), in which  $\dot{m}_h$  is directly measured using the calibrated piston exit venturi as previously discussed. The fluid density,  $\rho_{\text{sw}}$ , is calculated using the equation of state with the measured pressure and temperature upstream of the swirler. This calculation is consistent with that used in processing the survey data from the atmospheric test facility. The resulting total pressure profile is shown in Fig. 16(a) along with the secondary velocity vectors.

The maximum variation in  $p_{01}$  over the turbine inlet plane was measured to be  $\pm 0.35\%$ . This variation is notably lower than the  $\pm 1.5\%$  variation reported by Qureshi and Povey [4] downstream of a similar swirler design, which is consistent with the difference in swirl number (which was greater in Ref. [4]).

The dimensionless  $T_{0,\text{eff}}$  profile shown in Fig. 15 can be converted to total temperature,  $T_0$ , by rearranging Eq. (8) and using the measured hot and cold stream total temperatures,  $T_{0h}$  and  $T_{0c}$ , listed in Table 3. Similarly, to assess the  $T_0$  profile that would have been generated had the design supply temperatures listed in Table 2 been achieved, the  $T_{0,\text{eff}}$  profile can be converted to total temperature using  $T_{0h} = 530$  K and  $T_{0c} = 290$  K. The resulting  $T_0$  profile is shown in Fig. 16(b).

It is noteworthy that the increased  $T_{0h}$  at this condition would cause an increase in  $T_{01}$ , which would lead to a reduction in total turbine mass flow rate ( $\dot{m}_h + \dot{m}_c$ ). For a fixed  $\dot{m}_c$ , this leads to a reduction in  $\dot{m}_h$ , which can be accounted for in the calculation of  $T_{01}$ . Since the total turbine mass flow rate is set by the near-choked NGV and  $\dot{m}_c$  is independently set,  $\dot{m}_h$  can be iteratively

calculated assuming fixed NGV capacity. This calculation results in  $\dot{m}_h = 18.33 \text{ kg s}^{-1}$ , which is approximately 4% below the average condition achieved during commissioning (listed in Table 3).

Figure 17 shows the radial profiles of  $p_{01}/\bar{p}_{01}$  and  $T_{01}/\bar{T}_{01}$  obtained via circumferentially area-averaging the 2D profiles shown in Fig. 16 and normalizing by the mass-mean values. The radial variation in  $p_{01}$  is approximately  $\pm 0.2\%$  of the mass-mean value while the radial variation in the  $T_0$  profile is more pronounced. The maximum and minimum values of  $T_{01}^{\text{radial}}/\bar{T}_{01}$  are 1.102 and 0.830, respectively, which compare very well with the target values of 1.085 and 0.840. Comparing these values to the equivalent for  $T_{01}^{\text{circ}}/\bar{T}_{01}$  (maximum 1.068 and minimum 0.999) quantifies the strength of the radial nonuniformity relative to the circumferential nonuniformity. A characteristic of lean-burn combustor exit profiles is that this ratio is relatively high (i.e., the total temperature nonuniformity is primarily radial).

A rich-burn (EOTDF) combustor simulator (producing a more severe radial temperature nonuniformity but no swirl) was developed for previous studies in the OTRF [3]. The target total temperature profile for the rich-burn combustor simulator had maximum and minimum values of  $T_{01}^{\text{radial}}/\bar{T}_{01}$  of 1.124 and 0.720, respectively; measurements in the OTRF indicated that a maximum value of approximately 1.18 was achieved. These temperature ratios indicate more severe nonuniformity than those achieved by the present lean-burn combustor simulator, as expected from an engine-representative rich-burn profile. The measured radial profile produced by the rich-burn combustor simulator is shown in Fig. 17(b) for comparison with the present lean-burn profile.

## Impact of Nonuniform Inlet Flow on Nozzle Guide Vane Aerodynamics: Computational Fluid Dynamics and Experiment

We now compare the measured and predicted NGV surface static pressure distributions (NGV from LEMCOTEC HP turbine tested in the OTRF) with uniform inlet conditions and with the combustor simulator installed.

**Numerical Setup.** ANSYS CFX was used to perform 1.5-stage Reynolds-averaged Navier-Stokes (RANS) simulations. The  $k - \omega$  shear stress transport model was employed for turbulence closure. The LEMCOTEC turbine blade-count ratio of 2.3:1 permitted a periodic computational domain covering only 18 deg circumferentially, equal to a single combustor simulator pitch. The same block-structured mesh was used for simulations with uniform and nonuniform inlet conditions. The NGV mesh was generated using the Rolls-Royce in-house Parametric Design Rapid Meshing system. Two NGV passages were modeled, each

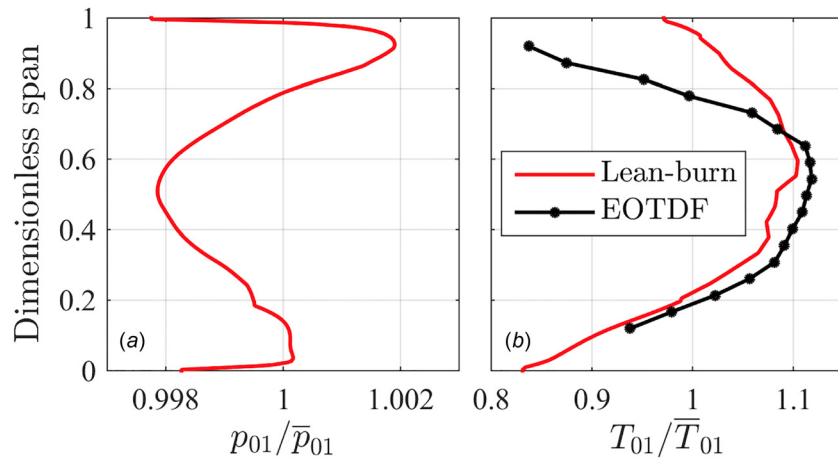


**Fig. 17 Radial profiles at turbine inlet, normalized by their mass-mean values: (a) total pressure and (b) total temperature from the lean-burn combustor simulator (scaled using the design temperatures  $T_{0h} = 530$  K and  $T_{0c} = 290$  K) and previous rich-burn (EOTDF) combustor simulator**

with a total of  $4.9 \times 10^6$  elements and with  $y^+ < 1$  on all wall surfaces. The downstream rotor and IP vane mesh domains were connected via steady mixing-plane interfaces. Both measurements and predictions presented in this paper were obtained without NGV film cooling.

**Boundary Conditions.** With uniform inlet conditions, the total temperature and total pressure at the turbine inlet plane were set uniformly at the measured values of 475 K and 8.5 bar. The flow angles at this plane were defined as axial and turbulence intensity was set at 10% based on hot-wire traverse measurements conducted downstream of the turbulence bars at atmospheric conditions [27]. With nonuniform inlet conditions, 2D profiles of total pressure and total temperature were imposed as shown in Fig. 16, while yaw and pitch angle profiles were imposed as shown in Fig. 7. The inlet turbulence intensity was set to 10%, based on measurements presented by Beard et al. [16] (measurements conducted downstream of similar swirlers employed in a previous OTRF campaign).

For both simulations, an exit boundary condition was imposed at the IP vane outlet and was defined as a linearly varying radial profile of static pressure. Values were set as the circumferentially average of measurements from nine static pressure tapings on each endwall surface distributed across one IP vane pitch and located at the same axial plane in the OTRF.

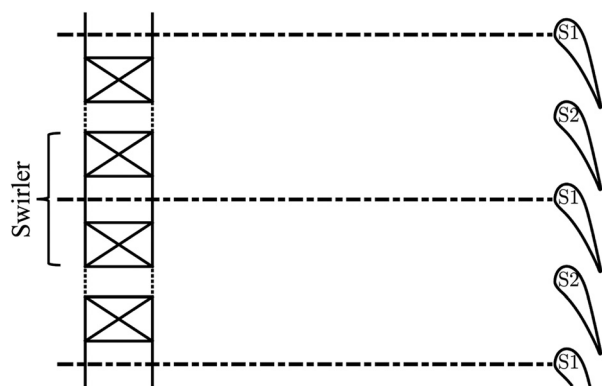


**Fig. 18 Schematic of swirler and NGV clocking positions (to scale)**

**Measurement and Prediction of Nozzle Guide Vane Loading Distribution.** Three separate uncooled NGVs were instrumented with over a total of 50 static pressure tapings (CNC-drilled with 1 mm diameter) at 10%, 50%, and 90% radial span. Pneumatic lines connected the tapings to pressure transducers with nominal uncertainty of  $\pm 0.1\%$  (to 95% confidence).

The 2:1 ratio of swirlers to NGVs meant that measurements were required at two vane positions in order to fully characterize the impact on NGV loading. Therefore, with nonuniform inlet conditions, measurements were conducted on vanes at two clocking positions with respect to the swirlers, denoted as S1 and S2. The clocking configuration is illustrated schematically in Fig. 18. In position S1, the NGV LE is aligned with a swirler centerline while in position S2, the LE is aligned midway between two swirlers.

The results with uniform and nonuniform inlet conditions are compared in Fig. 19. The measured pressures have been normalized by the mass-mean total pressure at the turbine inlet plane. All experimental data have been averaged over at least two runs. Data from different runs, when normalized by the turbine inlet total pressure, were observed to collapse with excellent agreement.

Measurements and predictions at 10% span show increased loading on the forward part of the vane ( $0.5 < x/C_{ax} < 1$ ) with nonuniform inlet conditions, which can be attributed to positive incidence near the hub. This change is reflected by increased acceleration on the early half of the vane suction side (SS). The magnitude of this effect is comparable on both vanes, despite only vane S1 being aligned with the swirler centerline. On the vane pressure side (PS), excellent agreement is observed between measurements and predictions, with neither showing significant sensitivity to the inlet nonuniformity. On the SS, some small discrepancies are seen. In particular, the static pressure is under-predicted on the late SS ( $0.75 < x/C_{ax} < 1$ ). This is thought to result from small differences between the build geometry in the experiment and the CFD model, which can have large impact near the vane throat; the use of a mixing plane between the vane and rotor may also contribute to this discrepancy (unsteady effects are not captured). Nevertheless, the effect of the nonuniform inlet condition appears well captured by the RANS model.

At 90% span, measurements and predictions show reduced loading on the forward part of the vane with nonuniform inlet conditions, which can be attributed to negative incidence near the casing. This change is reflected by the reduced acceleration (increased static pressure) on the early SS. This effect is of similar magnitude on both vanes. (Several measurements on the early PS

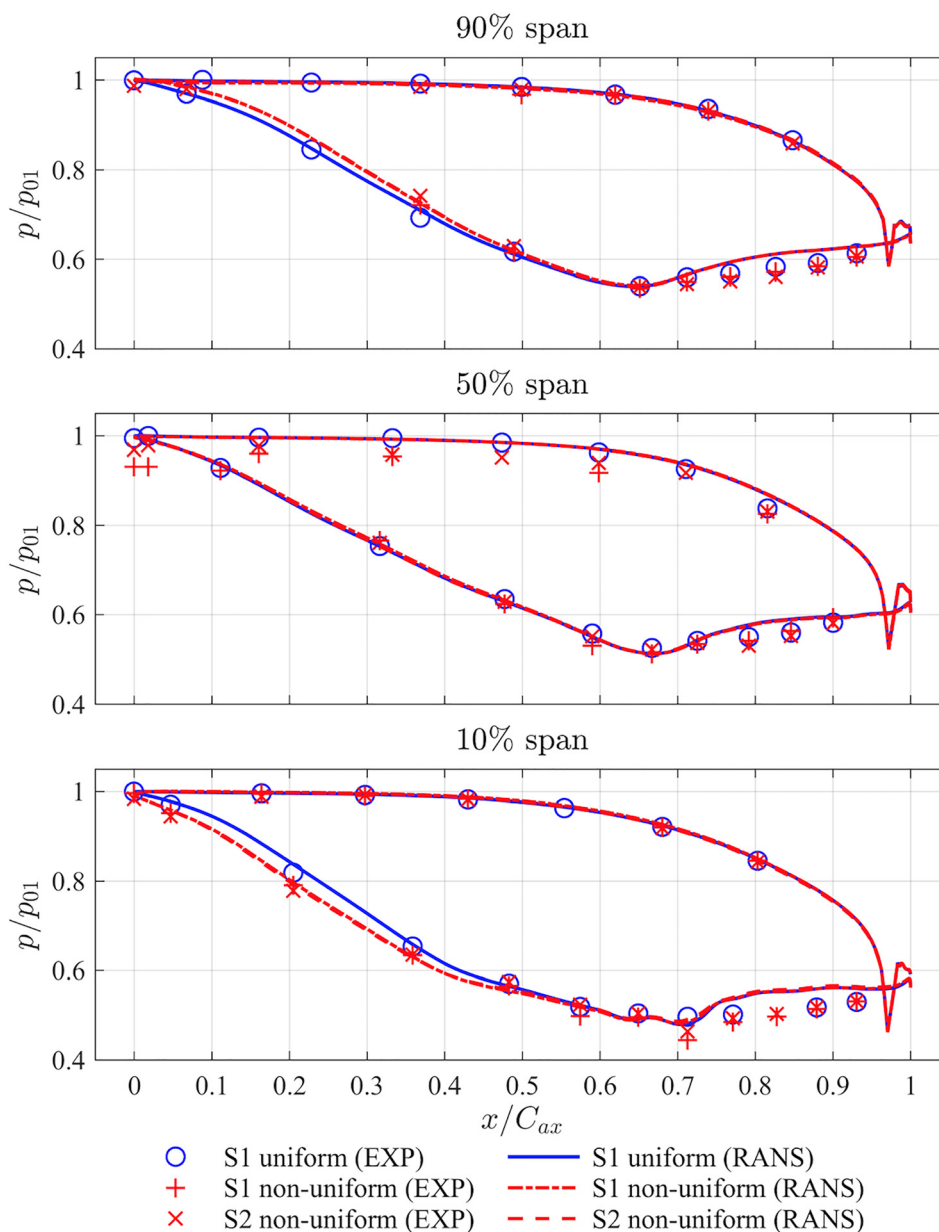


**Fig. 19 Experimental measurements and CFD predictions of LEMCOTEC NGV loading with uniform and engine-representative lean-burn (nonuniform) inlet conditions**

and SS with nonuniform inlet conditions were rejected due to damaged pressure tappings.) In similarity to the results at 10% span, both measurements and predictions at the LE virtually overlay. On the PS, measurements and predictions show excellent agreement, with neither showing sensitivity to the inlet nonuniformity.

At 50% span, the measured static pressures on the along the first 60%  $C_{ax}$  on the PS appear reduced with nonuniform inlet conditions. Furthermore, the pressure measured at the LE of vane S1 is 3.9% lower than for vane S2. These measurements seem to be consistent with the presence of the swirler loss core. Vane S1 is expected to experience slightly lower surface pressure near its LE than vane S2, given its more direct alignment with the swirler vortex core. Surprisingly, however, the difference in pressure is an order of magnitude greater than the variation in  $p_{01}$  ( $\pm 0.35\%$ ) over the turbine inlet plane—see Fig. 16. Indeed, the CFD-predicted static pressures with nonuniform inlet conditions (in which the  $p_{01}$  profile shown in Fig. 16 is imposed at inlet)

virtually collapse on both vanes at the same values as predicted with uniform inlet conditions.

The discrepancy between measured and predicted surface pressures on the vane midspan LEs would appear to suggest that the  $p_{01}$  profile shown in Fig. 16(a)—which is based on measurements from the atmospheric test facility scaled to OTRF conditions—does not accurately represent the true total pressure profile at turbine inlet in the OTRF: the total pressure deficit at the vortex core is lower in the CFD boundary condition than in the OTRF. Since previous experimental and computational results have indicated that the separated flow downstream of the combustor simulator is Reynolds number-independent so far as total pressure loss is concerned, skepticism is maintained about whether the apparent deficit in the vane surface pressure measurements is due to a real effect or an unknown measurement error. Nevertheless, the good agreement between the measured and predicted vane loading changes at 10% and 90% span indicates that such an effect did not significantly alter the generated swirling velocity profile.



At all three span locations, both measurements and predictions show that the loading distribution between  $0.5 < x/C_{ax} < 1$  is largely unchanged with the introduction of nonuniform inlet conditions. The insensitivity of the late PS and SS distributions to swirl can be attributed to the acceleration through the passage, which acts to attenuate the swirl strength. The measurements and predictions of vane aerodynamics show generally good agreement (except, as discussed, at midspan on the early PS), and both capture the key effects expected with the introduction of swirl. It is therefore concluded that the combustor simulator performed successfully in the OTRF and that the boundary condition imposed at turbine inlet is appropriate.

## Conclusions

A new nonreacting lean-burn combustor simulator was implemented in the OTRF, a short-duration rotating turbine facility. To the best of our knowledge, this is the first implementation of a combustor simulator producing both hot-streak and swirl profiles simultaneously in a rotating turbine facility. Total temperature survey measurements were conducted downstream of the simulator at turbine inlet. The results showed that a strong radial and weak circumferential nonuniformity (characteristic of lean-burn combustor exit flows) was successfully produced.

A significant drop in temperature of the hot stream was measured across the simulator; this was caused by convective heat transfer to the metal components. The effect of this heat loss was to reduce the mass-mean total temperature at turbine inlet significantly (by approximately 6% of the design value). In future studies, this heat loss should be accounted for by increasing the swirler-upstream total temperature via modification of the piston compression process.

More detailed survey measurements of total temperature, total pressure, and swirl angles were conducted downstream of the simulator installed in a separate (blowdown) test facility exhausting to atmosphere. The results showed that the flow field produced at turbine inlet possessed the key engine-representative features, including a well-defined vortex core, a total temperature profile with strong radial and weak circumferential nonuniformity, and the correct nonuniform total pressure profile.

A URANS model was used to predict the flow at simulator exit at both atmospheric and OTRF conditions. The swirl profile predictions at atmospheric conditions validated well against the survey measurements from the atmospheric test facility, while the temperature profiles validated poorly. This discrepancy was partly attributed to the small hot/cold stream temperature difference in the atmospheric test facility. The predictions at OTRF and atmospheric conditions showed virtually no difference, despite the increased Reynolds number.

The survey data acquired in both test facilities were extrapolated (using URANS-predicted radial trends) to cover the full span, scaled to the design OTRF conditions, and imposed as boundary conditions at inlet to a RANS model of the 1.5-stage LEMCOTEC turbine. Measurements and predictions of first vane loading distributions were used to validate the imposed swirl and total pressure profiles (which were not surveyed in the OTRF due to probe access limitations). Generally good agreement was found, except for where the effect of the swirler vortex core was prominent: measurements showed an order-of-magnitude greater vane surface pressure deficit near midspan than expected based on the scaled survey results from the atmospheric facility. This result was surprising, as previous experimental and computational results have indicated that the total pressure loss characteristics of the separated flow downstream of the combustor simulator are Reynolds number-independent; there remains uncertainty in whether the apparent deficit in the vane surface pressure measurements is due to a real effect or an unknown measurement error.

The data presented in this paper will provide a baseline for subsequent experimental and computational studies of the LEMCOTEC turbine with lean-burn inlet conditions in Oxford. It is hoped

that the results of this paper will also provide helpful guidelines for future experimental studies of lean-burn combustor-turbine interaction in transient turbine test facilities elsewhere.

## Acknowledgment

The authors would like to acknowledge the financial support provided by the European Commission and its partners through the LEMCOTEC project (EU Grant Number 283216) within the Seventh Framework Programme, and that provided by Rolls-Royce plc. The authors would also like to thank S. Chana and T. Godfrey of the University of Oxford for their assistance in running the OTRF and constructing the measurement instrumentation.

## Funding Data

- European Commission and its partners through the LEMCOTEC project (Grant No. 283216).

## Nomenclature

$A_w$	= combustor simulator wetted surface area, $m^2$
$A_{hole}$	= choked casing feed hole area, $m^2$
$A_{Sw}$	= planar area based on swirler passage outer radius ( $\pi r_{Sw}^2$ ), $m^2$
$c_p$	= Specific heat capacity, $J kg^{-1} K^{-1}$
$C_{ax}$	= NGV axial chord, m
$C_d$	= discharge coefficient of choked casing feed holes
$d_{Sw}$	= outer diameter of swirler passage ( $2r_{Sw}$ ), m
$h$	= heat transfer coefficient, $W m^{-2} K^{-1}$
$\dot{m}$	= mass flow rate, $kg s^{-1}$
$M$	= Mach number
$N$	= turbine rotational speed, rpm
$n_{hole}$	= number of choked casing feed holes
$p$	= pressure, bar
$Pr$	= Prandtl number, $\mu c_p/k$
$q$	= dynamic pressure, bar
$R$	= specific gas constant for air, $J kg^{-1} K^{-1}$
$r_{Sw}$	= outer radius of swirler passage, m
$Re$	= Reynolds number
$Re_{NGV}$	= Reynolds number based on $C_{ax}$
$Re_{Sw}$	= Reynolds number based on $d_{Sw}$
$S1$	= NGV aligned with swirler centerline
$S2$	= NGV aligned midway between swirler centerlines
$T$	= temperature, K
$T_{0,eff}$	= total temperature effectiveness
$u$	= velocity, $m s^{-1}$
$x$	= axial coordinate, m
$y^+$	= dimensionless wall coordinate

## Greek Symbols

$\alpha$	= yaw angle, deg
$\beta$	= pitch angle, deg
$\gamma$	= ratio of specific heat capacities
$\Gamma$	= flow capacity, $kg s^{-1} K^{1/2} Pa^{-1}$
$\zeta_{Sw}$	= swirler total pressure loss coefficient ( $p_{0Sw} - p_0$ )/ $q_{Sw}$
$\Theta$	= dimensionless total temperature drop across combustor simulator ( $T_{01} - T_{0Sw}$ )/( $T_w - T_{0Sw}$ )
$\mu$	= dynamic viscosity, Pa-s
$\rho$	= density, $kg m^{-3}$

## Subscripts

0	= gas stagnation condition
1	= turbine inlet
2	= NGV exit
4	= IP vane exit

$c$  = cold stream  
 $h$  = hot mainstream  
 $w$  = wall

## Superscripts and Annotations

$\bar{(\quad)}$  = mass-averaged  
 $[\quad]_{\text{circ}}$  = circumferential profile (radially averaged)  
 $[\quad]_{\text{radial}}$  = radial profile (circumferentially averaged)

## Abbreviations

ATM = atmospheric  
 CFD = computational fluid dynamics  
 EOTDF = enhanced overall temperature distortion function  
 HP = high pressure  
 IP = intermediate pressure  
 LE = leading edge  
 LEMCOTEC = low-emissions core engine technologies  
 NGV = nozzle guide vane  
 OTDF = overall temperature distortion function  
 OTRF = Oxford Turbine Research Facility  
 PS = pressure side  
 RANS = Reynolds-averaged Navier-Stokes  
 URANS = unsteady Reynolds-averaged Navier-Stokes  
 SS = suction side  
 TE = trailing edge  
 2D = two-dimensional

## References

- [1] Povey, T., and Qureshi, I., 2009, "Developments in Hot-Streak Simulators for Turbine Testing," *ASME J. Turbomach.*, **131**(3), p. 031009.
- [2] Chana, K. S., Hurion, J. R., and Jones, T. V., "The Design, Development and Testing of a Non-Uniform Inlet Temperature Generator for the QinetiQ Transient Turbine Research Facility," *ASME Paper No. GT2003-38469*.
- [3] Povey, T., and Qureshi, I., 2008, "A Hot-Streak (Combustor) Simulator Suited to Aerodynamic Performance Measurements," *Proc. Inst. Mech. Eng., Part G*, **222**(6), pp. 705–720.
- [4] Qureshi, M. I., and Povey, T., 2011, "A Combustor-Representative Swirl Simulator for a Transonic Turbine Research Facility," *Proc. Inst. Mech. Eng., Part G*, **225**(7), pp. 737–748.
- [5] Povey, T., Chana, K. S., and Jones, T. V., 2003, "Heat Transfer Measurements on an Intermediate-Pressure Nozzle Guide Vane Tested in a Rotating Annular Turbine Facility, and the Modifying Effects of a Non-Uniform Inlet Temperature Profile," *Proc. Inst. Mech. Eng., Part A*, **217**(4), pp. 421–431.
- [6] Chana, K. S., and Jones, T. V., 2003, "An Investigation on Turbine Tip and Shroud Heat Transfer," *ASME J. Turbomach.*, **125**(3), pp. 513–520.
- [7] Povey, T., Chana, K. S., Jones, T. V., and Hurion, J., 2007, "The Effect of Hot-Streaks on HP Vane Surface and Endwall Heat Transfer: An Experimental and Numerical Study," *ASME J. Turbomach.*, **129**(1), pp. 32–43.
- [8] Salvadori, S., Montomoli, F., Martelli, F., Adami, P., Chana, K. S., and Castillon, L., 2011, "Aerothermal Study of the Unsteady Flow Field in a Transonic Gas Turbine With Inlet Temperature Distortions," *ASME J. Turbomach.*, **133**(3), p. 031030.
- [9] Simone, S., Montomoli, F., Martelli, F., Chana, K. S., Qureshi, I., and Povey, T., 2012, "Analysis on the Effect of a Nonuniform Inlet Profile on Heat Transfer and Fluid Flow in Turbine Stages," *ASME J. Turbomach.*, **134**(1), p. 011012.
- [10] Qureshi, I., Smith, A. D., Chana, K. S., and Povey, T., 2012, "Effect of Temperature Nonuniformity on Heat Transfer in an Unshrouded Transonic HP Turbine: An Experimental and Computational Investigation," *ASME J. Turbomach.*, **134**(1), p. 011005.
- [11] Qureshi, I., Beretta, A., Chana, K., and Povey, T., 2012, "Effect of Aggressive Inlet Swirl on Heat Transfer and Aerodynamics in an Unshrouded Transonic HP Turbine," *ASME J. Turbomach.*, **134**(6), p. 061023.
- [12] Qureshi, I., Smith, A. D., and Povey, T., 2012, "HP Vane Aerodynamics and Heat Transfer in the Presence of Aggressive Inlet Swirl," *ASME J. Turbomach.*, **135**(2), p. 021040.
- [13] Johansson, M., Povey, T., Chana, K. S., and Abrahamsson, H., 2016, "Effect of low- $\text{NO}_x$  Combustor Swirl Clocking on Intermediate Turbine Duct Vane Aerodynamics With an Upstream High Pressure Turbine Stage—an Experimental and Computational Study," *ASME J. Turbomach.*, **139**(1), p. 011006.
- [14] Beard, P. F., Povey, T., and Ireland, P. T., 2008, "Mass Flow Rate Measurement in a Transonic Turbine Test Facility With Temperature Distortion and Swirl," *Flow Meas. Instrum.*, **19**(5), pp. 315–324.
- [15] Beard, P. F., Smith, A., and Povey, T., 2012, "Impact of Severe Temperature Distortion on Turbine Efficiency," *ASME J. Turbomach.*, **135**(1), p. 011018.
- [16] Beard, P. F., Smith, A. D., and Povey, T., 2013, "Effect of Combustor Swirl on Transonic High Pressure Turbine Efficiency," *ASME J. Turbomach.*, **136**(1), p. 011002.
- [17] Khanal, B., He, L., Northall, J., and Adami, P., 2013, "Analysis of Radial Migration of Hot-Streak in Swirling Flow Through High-Pressure Turbine Stage," *ASME J. Turbomach.*, **135**(4), p. 041005.
- [18] Hall, B. F., Chana, K. S., and Povey, T., 2014, "Design of a Non-Reacting Combustor Simulator With Swirl and Temperature Distortion With Experimental Validation," *ASME J. Eng. Gas Turbines Power*, **136**(8), p. 081501.
- [19] Hall, B. F., and Povey, T., 2015, "Experimental Study of Non-Reacting Low  $\text{NO}_x$  Combustor Simulator for Scaled Turbine Experiments," *ASME Paper No. GT2015-43530*.
- [20] Koupper, C., Caciolli, G., Gicquel, L., Duchaine, F., Bonneau, G., Tarchi, L., and Facchini, B., 2014, "Development of an Engine Representative Combustor Simulator Dedicated to Hot-Streak Generation," *ASME J. Turbomach.*, **136**(11), p. 111007.
- [21] Bacci, T., Caciolli, G., Facchini, B., Tarchi, L., Koupper, C., and Champion, J. L., 2015, "Flowfield and Temperature Profiles Measurements on a Combustor Simulator Dedicated to Hot-Streaks Generation," *ASME Paper No. GT2015-42217*.
- [22] Hilditch, M. A., Fowler, A., Jones, T. V., Chana, K. S., Oldfield, M. L. G., Ainsworth, R. W., Hogg, S. I., Anderson, S. J., and Smith, G. C., 1994, "Installation of a Turbine Stage in the Pyestock Isentropic Light Piston Facility," *ASME Paper No. 94-GT-277*.
- [23] Beard, P. F., Adams, M. G., Stokes, M. R., Wallin, F., Cardwell, D. N., Povey, T., and Chana, K. S., 2019, "The LEMCOTEC  $1\frac{1}{2}$  Stage Film-Cooled HP Turbine: Design, Integration, and Testing in the Oxford Turbine Research Facility," *Paper No. ETC201-216*.
- [24] Kilik, E., 1976, "The Influence of Swirler Design Parameters on the Aerodynamics of Downstream Recirculation Region," Ph.D. thesis, Cranfield University, Cranfield, UK.
- [25] Sarpkaya, T., 1971, "Vortex Breakdown in Swirling Conical Flows," *AIAA J.*, **9**(9), pp. 1792–1799.
- [26] Hall, B. F., and Povey, T., 2017, "The Oxford Probe: An Open Access Five-Hole Probe for Aerodynamic Measurements," *Meas. Sci. Technol.*, **28**(3), p. 035004.
- [27] Hall, B. H., 2015, "Combustor Simulators for Scaled Turbine Experiments," DPhil thesis, University of Oxford, Oxford, England.